WEP Warwick Evans Publishing

International Journal of Natural Resources and Environmental Studies

ISSN: 3006-2012 (Print), ISSN: 3006-0834 (Online) | Volume 8, Number 5, Year 2026
DOI: https://doi.org/10.62051/ijnres.v8n5.08
Journal homepage: https://wepub.org/index.php/IJNRES/index

A Study on Structural Parameters of Solid Potassium Salt Mines

Yukun Zhang

School of Energy, Henan University of Science and Technology, Luoyang, China

ABSTRACT

To ensure the safety and efficiency of solid potassium salt mine mining, this paper focuses on the research of stope structural parameters, including stope room span, roof safety thickness, and stope layout form. Based on the equilibrium arch theory and simply supported beam theory, the limit span of the stope room is analyzed and calculated, and the reasonable room span is determined by combining mining technology and safety requirements. Using the elastic mechanics thin plate theory and H. Tresca yield criterion, the safety thickness of the stope roof is calculated to ensure the overall stability of the stope during mining. Two stope layout schemes (uniform layout of rooms and pillars, interval large pillars with equal-width rooms) are designed, and the parameters of each scheme are calculated and compared from the aspects of pillar safety factor and recovery rate. The research results show that the reasonable room span of the carnallite ore layer is 8m, the safe thickness of the roof isolation layer should be more than 7.5m, and the interval large pillar layout scheme has higher recovery rate while ensuring safety, which can provide a theoretical basis and engineering reference for the design and construction of solid potassium salt mines.

KEYWORDS

Solid potassium salt mine; Stope structural parameters; Room span; Roof safety thickness; Stope layout.

1. INTRODUCTION

Solid potassium salt is an important strategic resource, which is widely used in chemical industry, agriculture, medicine and other fields. With the increasing demand for potassium salt resources, the mining depth and scale of potassium salt mines are constantly expanding, and the problem of stope stability has become increasingly prominent. The stope structural parameters, including room span, roof safety thickness and stope layout form, are the key factors affecting the stope stability and mining efficiency. Reasonable stope structural parameters can not only ensure the safety of mining operations, but also improve the resource recovery rate and reduce mining costs.

At present, there are many studies on stope structural parameters of metal mines and coal mines, but the research on solid potassium salt mines, which have the characteristics of soft rock and easy deformation, is relatively insufficient. Therefore, it is of great practical significance to carry out the research on stope structural parameters of solid potassium salt mines. Niu Haiping et al.[1] determined the optimal width of support pillars in complex structures; Sun Lihui et al.[2] used theoretical calculations and numerical simulations to derive the optimal width of support pillars; Ahmad Mahmood et al. 3 developed two models for predicting pillar instability by employing random forest and C4.5 decision tree algorithms, respectively, based on four parameters: pillar width, height, strength, and stress. Performance metrics such as accuracy, precision, recall, F-measure, and the Matthews correlation coefficient indicate that both models demonstrate reasonable accuracy.; Ma

Jianwen et al.4 employed theoretical analysis, numerical simulation, and in-mine pressure measurement methods to determine the reasonable width of narrow coal pillars; Peng Linjun 5 et al. investigated the issue of in-mine pressure control in narrow coal pillar longwall goaf roadways in deep, high-seam longwall mining faces and optimized the dimensions of the coal pillars; Rui Shaoge 6 et al. determined the reasonable width to be retained based on the patterns of displacement and plastic zone changes, and identified the optimal solution through a comparison of support parameters. Reinforcing coal pillars can effectively enhance their strength; Lan Changjin et al.[7] demonstrated the stability of unstable coal pillars after artificial reinforcement; Li Jian[8] et al. verified the strengthening effect of FRP strips on coal pillars; Gu Changwan[9] et al. conducted experimental studies on the load-bearing performance of coal pillars left in longwall face backfill under the reinforcement of through-bolts, analyzing the effects of different through-bolt reinforcement methods on the failure modes, load-bearing capacity, and deformation patterns of coal pillars, as well as the resulting stress variations in the through-bolts. Wattimena R K et al. 10 used the logistic method to generate probability contour maps for different stability levels of mine pillars based on two sets of parameters—pillar geometry and rock strength—in order to evaluate the condition of the pillars..

This paper takes the solid potassium salt mine as the research object, combines theoretical analysis and calculation, studies the key structural parameters of the stope, and puts forward reasonable design schemes, so as to provide support for the safe and efficient mining of the mine. The introduction provides background information and indicates the purpose of the manuscript, and places the work in the perspective of relevant research.

2. ANALYSIS OF STOPE ROOM SPAN

2.1. Equilibrium Arch Theory

M.M. Protoyanov from Russia proposed the equilibrium arch theory, also known as "Protodyakonov's theory", after a large number of model tests and theoretical derivations. The key point of this theory is that under a certain burial depth, after the excavation of a tunnel or other underground caverns, if support is not carried out in time, the rock mass at the top of the cavern will continue to collapse to form an arch, also known as a caving arch.

Initially, this arch is unstable; if the side walls of the cavern are stable, the arch height will continue to increase with collapse; on the contrary, if the side walls are also unstable, both the arch span and the arch height will increase simultaneously. When this collapse changes the shape of the cavern to a certain extent, it will no longer develop, and a certain range of self-stable equilibrium arch will appear in the caving arch. At this time, the support structure only needs to bear the weight of the rock and soil in the equilibrium arch to ensure the stability of the cavern.Figure 1 shows a schematic diagram of the Pultzi arch.

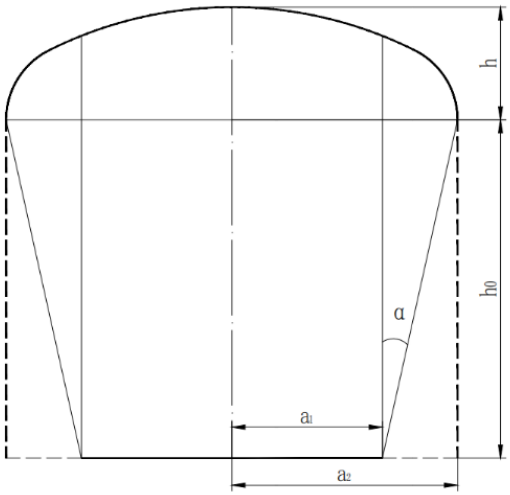

Figure 1 Schematic Diagram of the Pruett Arch

If the side walls of the cavern are unstable, the half-span of the cavern will expand from a1 to a2 , as shown in the figure. At this time, the rock mass of the side walls will be in a state of limit equilibrium (plastic equilibrium), the angle between the fracture line and the vertical line is α=45°-φ/2, and the span of the pressure arch should be determined according to the boundary of the fracture lines on both sides.

$$2a_2 = 2a_1 + 2h_0 \cdot \tan\alpha \tag{1}$$

In the formula,a1 is the half-span of the cavern, m;a2 is the half-span of the caving arch, m;h0 is the height of the cavern, m;φ is the internal friction angle of the rock mass, °.

$$h = \frac{a_2}{f} \tag{2}$$

In the formula,h is the height of the equilibrium arch, m; f is the Protodyakonov coefficient of the rock mass.

For soft rock mass,f can be taken as:

$$f = \tan\varphi + \frac{c}{\sigma_c} \tag{3}$$

In the formula,c is the cohesion of the rock mass, MPa; σc is the uniaxial compressive strength of the rock, MPa.

2.2. Simply Supported Beam Theory

If the room span is too large, the roof rock layer in the center of the room will produce separation, bending, fracture or caving under the action of tensile stress. Therefore, assuming that the statistical height of caving is the height of the rock beam, according to material mechanics, the roof of the goaf is assumed to be a simply supported rock beam force model at both ends. The limit span of the roof at this time is obtained as:

$$l_{\max} = \sqrt{\frac{4h_1 \cdot \sigma_{mt}}{3\gamma}} \tag{4}$$

In the formula,lmax is the limit span of the roof, m;h1 is the height of the rock beam, m;σmt is the tensile strength of the rock mass, MPa;γ is the bulk density of the rock mass, MN/m³.

2.3. Analysis of Room Span Based on Equilibrium Arch and Simply Supported Beam Theories

Through the above relevant theoretical analysis, assuming that the caving height is the height of the caving arch, that is, , then from the simultaneous equations (1), (2), and (4), we can get:

$$l_{\max} = \sqrt{\frac{4\sigma_{mt}\left[a_1 + h_0 \cdot \tan\alpha\right]}{3\gamma\left(\tan\varphi + \frac{c}{\sigma_c}\right)}} \tag{5}$$

In the formula, the meanings of the symbols are the same as above.

According to the equilibrium arch theory, the limit span of the room lmax=2a1 , so the limit span of the room can be obtained:

$$2a_1 = \frac{\sigma_{mt} + \sqrt{\sigma_{mt}{}^2 + 12\gamma \cdot f \cdot h_0 \cdot \tan\varphi}}{3\gamma \cdot f} \tag{6}$$

The corresponding rock mass parameters are substituted into formula (6), and the calculation results are shown in Table 1.

Table 1. Three Scheme comparing

Rock Layer	Tensile Strength of Rock Mass (MPa)	Bulk Density of Overlying Rock (MN/m³)	Protodyakonov Coefficient of Direct Roof Rock Mass	Room Span (m)
Carn-allite	0.109	0.022	0.815	8.20

The limit room span for ore layer mining is 8.20m. Considering the mining technology and safety of the ore layer comprehensively, the room span is selected as 8m.

3. COMPARATIVE ANALYSIS OF STOPE LAYOUT FORM PARAMETERS

3.1. Scheme 1: Uniform Layout of Rooms and Pillars

As mentioned earlier, the reasonable room span is 8m, and the pillar mining height is 7m. At present, in the design of room-and-pillar mines, the pillar safety factor is generally calculated by the following formula:

$$K = \frac{S_p}{\sigma_p} \tag{7}$$

In the formula,Sp is the pillar strength, Mpa;σp is the average pillar stress, Mpa.

According to the Bieniawski formula, the pillar strength calculation formula is:

$$S_p = S_t\left[0.64 + 0.36\left(\frac{W_p}{h}\right)\right]^{\alpha} \tag{8}$$

In the formula, St represents the compressive strength of the rock mass, MPa;Wp represents the width of the rock pillar,m; h represents the height of the rock pillar, m; α is a constant whose value depends on the aspect ratio of the rock pillar. When the aspect ratio is greater than 5, α=1.4; when the aspect ratio is less than 5, α=1.

After calculation, when the pillar width ranges from 7 to 11m, the corresponding safety factors are shown in Table 2.

Table 2. Calculation results of pillar safety factor (Scheme 1)

Uniaxial Compressive Strength of Ore Rock (MPa)	Pillar Height (m)	Room Width (m)	Pillar Width (m)	Pillar Safety Factor
9.3	7	8	7	1.077
9.3	7	8	8	1.213
9.3	7	8	9	1.347
9.3	7	8	10	1.480
9.3	7	8	11	1.611

Combined with on-site actual conditions and mining experience, the critical safety factor is selected as 1.35. It is calculated that when the pillar width reaches 10m, its safety factor can reach 1.35.Figure 2 shows a schematic diagram of the mining area for Scheme 1.Schematic diagram of the mining area for Scheme 1.

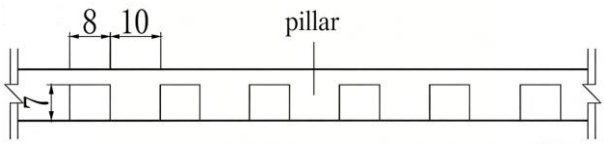

Figure 2 Schematic diagram of the mining area for Scheme 1

The recovery rate of this scheme is 44.44%. It should be noted that the calculation result here is the calculation of the block recovery rate by the area ratio method, which is different from the actual mining recovery rate.

3.2. Scheme 2: Interval Large Pillars with Equal-Width Rooms

Referring to the experience of stope layout in foreign potassium salt mines, by adopting the form of non-uniform pillar layout in the stope, the state where each pillar is under large stress during uniform pillar layout is transformed into local large pillars bearing most of the stress, while some small pillars undergo plastic failure, and stress transfer and stress release occur at the same time to ensure the overall stability of the stope.

3.2.1. Calculation of Stope Unit Width

According to the engineering geological data, the upper part of the carnallite ore layer is a 54m thick mudstone layer. Combined with the equilibrium arch theory, the height of the caving arch formed by lower mining should be less than the thickness of the roof mudstone ore layer of 54m.

Considering the safety factor comprehensively, 7.5m thick ore layer is reserved to avoid the influence of the caving arch, that is, the stope unit width is calculated with the caving arch height of 46.5m. According to formulas (1) and (2), the stope unit width should be 68m.

3.2.2. Calculation of Room Pillar Width

For the room pillars in the stope, the load they bear is equal to the weight of the overlying rock layer within the goaf range they support. The area supported by the pillars is the sum of the shared mining area and the area of the pillars themselves. Therefore, the average load of the pillars can be calculated as:

$$\sigma_v = \gamma h\left(1+2\frac{a_1}{l}\right) \tag{9}$$

In the formula,σv is the average pillar stress, Mpa;h is the thickness of the overlying rock layer, m;l is the room pillar width, m.

It should be specially pointed out that since only the broken rock mass in the caving arch will act on the room pillars, the thickness of the overlying rock layer h in the formula is taken as the height of the caving arch.

For the room pillars in the stope, due to their small width-height ratio, their stress state is approximately uniaxial stress state. Therefore, to ensure mining safety, the pillar safety factor is introduced as the ratio of the load borne by the pillar to its own strength. In this trial calculation, the pillar safety factor K=1.5 is taken, that is:

$$\sigma_{c\infty} = n\gamma h\left(1+2\frac{a_1}{l}\right) \tag{10}$$

$$l = \frac{2a_1 \cdot n\gamma h}{\sigma_{c\infty} - n\gamma h} \tag{11}$$

In the formula,σc∞ is the long-term uniaxial strength of the pillar rock mass, Mpa.

Table 3. Table for Calculating Mine Pillar Width

Rock Layer	Long-Term Uniaxial Strength of Rock Mass (MPa)	Room Half-Span (m)	Caving Arch Height	Room Pillar Width (m)
Carn-allite	4.8	0.022	41.5	3.76

To ensure safety, it is recommended that the width of the room pillars in the carnallite ore layer mining stope be 4m.

3.2.3. Calculation of Stope Unit Pillar

Referring to the coal mine yield pillar theory, it is considered that the soft rock pillar can be divided into two parts: yield zone and core zone, and the core zone is constrained by the yield zone. The core zone width of the stable coal pillar is approximately 65% of the coal pillar width, that is, the core zone ratio λ=0.65. From this conclusion, the design empirical formula of pillar width and yield zone width can be given:

$$\lambda = \frac{W_p - 2r_p}{W_p} > 0.65 \tag{12}$$

In the formula,λ is the core zone ratio;Wp is the limit pillar width, m;rp is the yield zone width, m.

When the stope side wall is not reinforced by anchoring and other support measures, the yield zone width of the pillar can be given by the following formula:

$$r_p = \frac{h_0 d\beta}{2\tan\varphi}\ln\left(1+\frac{\sigma_{zl}\tan\varphi}{c}\right)+\frac{d}{2}h_0\tan\varphi \tag{13}$$

In the formula,h0 is the pillar height, m;d is the mining disturbance factor,d=1.1~3.0;β is the lateral pressure coefficient at the interface between the yield zone and the core zone;σzl is the limit strength of the pillar, Mpa;φ is the internal friction angle of the rock mass, °;c is the cohesion of the rock mass, Mpa.

To give full play to the bearing capacity of the stope unit pillars, it is allowed to produce yield on both sides near the excavation surface to form a yield pillar bearing form.When the pillar is in the limit stress state, the plastic zone width is 5.51m, and the limit pillar width is 31.47m. Therefore, the corresponding stope unit pillar width is 32m.

In summary, the schematic diagram of the obtained stope structural parameters is shown in the figure 3.

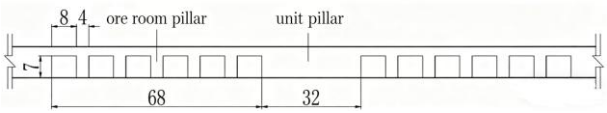

Figure 3 Schematic diagram of the mining area for Scheme 2

According to the estimation of the mining area ratio, the recovery rate of this scheme is 68.2% (supplemented according to the actual calculation logic of the scheme).

4. CONCLUSION

This paper focuses on the research of stope structural parameters of solid potassium salt mines, and draws the following main conclusions through theoretical analysis and calculation:

(1) Based on the equilibrium arch theory and simply supported beam theory, the limit span of the carnallite ore layer room is calculated as 8.20m, and the reasonable room span is determined as 8m by comprehensively considering the mining technology and safety.

(2) Using the elastic mechanics thin plate theory and H. Tresca yield criterion, the roof safety thickness is calculated. The results show that when the thickness of the reserved roof isolation layer is more than 7.5m, the safety factor is greater than 1, which can ensure the roof stability.

(3) Two stope layout schemes are designed. Scheme 1 (uniform layout of rooms and pillars) has a recovery rate of 44.44%, and the reasonable pillar width is 10m; Scheme 2 (interval large pillars with equal-width rooms) has a higher recovery rate (68.2%), and the recommended room pillar width is 4m, and the stope unit pillar width is 32m. Compared with Scheme 1, Scheme 2 has obvious advantages in resource recovery rate while ensuring safety. The research results can provide a theoretical basis and engineering reference for the safe and efficient mining of solid potassium salt mines. Future research can focus on the optimization of stope structural parameters under different mining conditions and the verification of field engineering.

REFERENCES

[1] Niu, H. P., Pan, K. R., Yu, W. D., et al. (2025). Mechanical characteristics of coal pillars in complex-structure coal seams and optimization of roadway surrounding rock stability. *Journal of Henan Polytechnic University (Natural Science)*, *44*(06), 118–126.

[2] Sun, L. H., Ding, B., Li, W. J., et al. (2023). Width optimization and application of narrow coal pillar in gob-side entry driven in thick coal seam in Luzigou Mine. *Journal of Mining & Safety Engineering*, *40*(6), 1151–1160.

[3] Ahmad, M., Al-Shayea, N. A., Tang, X., et al. (2020). Predicting the pillar stability of underground mines with random trees and C4.5 decision trees. *Applied Sciences-Basel*, *10*, 6486.

[4] Ma, J. W., Lyu, C. S., & Liao, Y. H. (2024). Research on the width of narrow coal pillars in goaf excavation roadway of fully mechanized caving face in inclined thick coal seam. *China Mining Magazine*, *33*(Sup.1), 317–322.

[5] Peng, L. J., Wu, J. Y., He, M. C., et al. (2024). Optimization of coal pillar and tunnel support for fully mechanized caving along gob in deep and extra thick coal seams. *Journal of Xi'an University of Science and Technology*, *44*(3), 563–574.

[6] Rui, S. G., Yao, W. J., Huang, X., et al. (2025). Rational width setting and support design for small coal pillars in trapezoidal asymmetric gob-side entry driving. *Journal of Safety Science and Technology*, *21*(8), 63–70.

[7] Lan, C. J. (2023). Stability demonstration of 0#, 0## and 1# pillars after reinforcement in the -240m level's East stope in Yushui sulfur-copper mine. *World Nonferrous Metals*, *(16)*, 148–151.

[8] Li, J., Bai, J. W., Feng, G. R., et al. (2024). Compressive performance of innovative reinforced pillars in closed/abandoned mines. *Journal of Central South University*, *31*(08), 2780–2793.

[9] Gu, C. W., Wang, B., Wang, J., et al. (2022). Research on bidirectional-reinforcement mechanism of narrow coal pillar of gob-side entry driving based on inflatable lock-type anchor. *Coal Science and Technology*, *50*(04), 106–116.

[10] Wattimena, R. K., Kramadibrata, S., Sidi, I. D., et al. (2013). Developing coal pillar stability chart using logistic regression. *International Journal of Rock Mechanics and Mining Sciences*, *58*, 55–60.

[11] Chen, S., Mulgrew, B., & Grant, P. M. (1993). A clustering technique for digital communications channel equalization using radial basis function networks. *IEEE Transactions on Neural Networks*, *4*, 570–578.

[12] Lucky, R. W. (1965). Automatic equalization for digital communication. *Bell System Technical Journal*, *44*(4), 547–588.

[13] Bingulac, S. P. (1994). On the compatibility of adaptive controllers. In *Proc. 4th Annu. Allerton Conf. Circuits and Systems Theory* (pp. 8–16). New York, NY, USA.

[14] Faulhaber, G. R. (1995). Design of service systems with priority reservation. In *Conf. Rec. 1995 IEEE Int. Conf. Communications* (pp. 3–8).

[15] Doyle, W. D. (1987). Magnetization reversal in films with biaxial anisotropy. In *1987 Proc. INTERMAG Conf.* (pp. 2.2-1–2.2-6).

[16] Juette, G. W., & Zeffanella, L. E. (1990, June 22–27). Radio noise currents in short sections on bundle conductors. Paper presented at the IEEE Summer Power Meeting, Dallas, TX, USA. Paper 90 SM 690-0 PWRS.

[17] Kreifeldt, J. G. (1989). An analysis of surface-detected EMG as an amplitude-modulated noise. Paper presented at the 1989 Int. Conf. Medicine and Biological Engineering, Chicago, IL, USA.

[18] Williams, J. (1993). *Narrow-band analyzer* (Doctoral dissertation). Harvard University, Cambridge, MA, USA.

[19] Kawasaki, N. (1993). *Parametric study of thermal and chemical nonequilibrium nozzle flow* (Master's thesis). Osaka University, Osaka, Japan.

[20] Wilkinson, J. P. (1990). Nonlinear resonant circuit devices. U.S. Patent 3,624,122.

[21] IEEE. (1969). *IEEE Standard 308: IEEE Criteria for Class IE Electric Systems*.

[22] ANSI. (1968). *ANSI Standard Y10.5-1968: Letter Symbols for Quantities*.

[23] Haskell, R. E., & Case, C. T. (1994). *Transient signal propagation in lossless isotropic plasmas* (Vol. 2). USAF Cambridge Research Laboratory, Cambridge, MA, USA. Rep. ARCRL-66-234 (II).

[24] Reber, E. E., Michell, R. L., & Carter, C. J. (1988, November). Oxygen absorption in the Earth's atmosphere. Aerospace Corp., Los Angeles, CA, USA. Tech. Rep. TR-0200 (420-46)-3.

[25] Vidmar, R. J. (1992, August). On the use of atmospheric plasmas as electromagnetic reflectors. *IEEE Transactions on Plasma Science*, *21*(3), 876–880. Retrieved from http://www.halcyon.com/pub/journals/21ps03-vidmar